Regularized Shock Filters and Complex Diffusion

Guy Gilboa[1], Nir A. Sochen[2], and Yehoshua Y. Zeevi[1]

[1] Department of Electrical Engineering, Technion – Israel Institute of Technology
Technion City, Haifa 32000, Israel
gilboa@tx.technion.ac.il, www.ee.technion.ac.il/∼ gilboa
zeevi@ee.technion.ac.il, www.ee.technion.ac.il/∼ zeevi
[2] Department of Applied Mathematics, University of Tel-Aviv, Tel-Aviv 69978, Israel
sochen@math.tau.ac.il, www.math.tau.ac.il/∼ sochen

Abstract. We address the issue of regularizing Osher and Rudin's shock filter, used for image deblurring, in order to allow processes that are more robust against noise. Previous solutions to the problem suggested adding some sort of diffusion term to the shock equation. We analyze and prove some properties of coupled shock and diffusion processes. Finally we propose an original solution of adding a complex diffusion term to the shock equation. This new term is used to smooth out noise and indicate inflection points simultaneously. The imaginary value, which is an approximated smoothed second derivative scaled by time, is used to control the process. This results in a robust deblurring process that performs well also on noisy signals.

Keywords: Shock filters, deblurring, denoising, image enhancement, complex diffusion, image features.

1 Introduction

1.1 Background

In the past decade there has been a growing amount of research concerning partial differential equations in the fields of computer vision and image processing. Applications, supported by rigorous theory, were developed for purposes such as image denoising and enhancement, segmentation, object tracking and many more. A review of topics in the subject can be seen in [14]; see [9] for more recent studies. The research is focused mostly on linear and nonlinear parabolic schemes of diffusion-type processes. In [11] Osher and Rudin proposed a hyperbolic equation called shock filter that can serve as a stable deblurring algorithm approximating deconvolution.

1.2 Problem Statement

The formulation of the shock filter equation is:

$$I_t = -|I_x|F(I_{xx}), \tag{1}$$

A. Heyden et al. (Eds.): ECCV 2002, LNCS 2350, pp. 399–413, 2002.

where F should satisfy $F(0) = 0, \quad F(s)\text{sign}(s) \geq 0$. Note: the above equation and all other evolutionary equations in this paper have initial conditions $I(x,0) = I_0(x)$ and Neumann boundary conditions ($\frac{\partial I}{\partial n} = 0$ where n is the direction perpendicular to the boundary).

Choosing $F(s) = \text{sign}(s)$ gives the classical shock filter equation:

$$I_t = -\text{sign}(I_{xx})|I_x|. \tag{2}$$

In the 2D case the shock filter equation is commonly generalized to:

$$I_t = -\text{sign}(I_{\eta\eta})|\nabla I|, \tag{3}$$

where η is the direction of the gradient.

The 1D process (Eq. 2) is approximated by the following discrete scheme:

$$I_i^{n+1} = I_i^n - \Delta t|DI_i^n|\text{sign}(D^2 I_i^n), \tag{4}$$

where

$$\begin{array}{l} DI_i^n \doteq m(\Delta_+ I_i^n, \Delta_- I_i^n)/h, \\ D^2 I_i^n \doteq (\Delta_+ \Delta_- I_i^n)/h^2, \end{array} \tag{5}$$

$m(x,y)$ is the minmod function:

$$m(x,y) \doteq \begin{cases} (\text{sign}x)\min(|x|,|y|) & \text{if } xy > 0, \\ 0 & \text{otherwise,} \end{cases}$$

and $\Delta_\pm \doteq \pm(u_{i\pm1} - u_i)$. The CFL condition in the 1D case is $\Delta t \leq 0.5h$.

The shock filter main properties are:

- Shocks develop at inflection points (second derivative zero-crossings).
- Local extrema remain unchanged in time. No new local extrema are created. The scheme is total variation preserving (TVP).
- The steady state (weak) solution is piece-wise constant (with discontinuities at the inflection points of I_0).
- The process approximates deconvolution.

Most rigorous analysis and proofs of these properties were based on the discrete scheme (Eq. 4).

As already noted in the original paper, any noise in the blurred signal will also be enhanced. As a matter of fact this process is extremely sensitive to noise. Theoretically, in the continuous domain, any white noise added to the signal may add an infinite number of inflection points, disrupting the process completely. Discretization may help somewhat, but in general the same sensitivity to noise occurs. In Fig. (1) we compare the process acting on a sine wave without noise and with very low additive white Gaussian noise (SNR=40dB). Clearly the signal in the noisy case is not enhanced and the process results mainly in noise amplification.

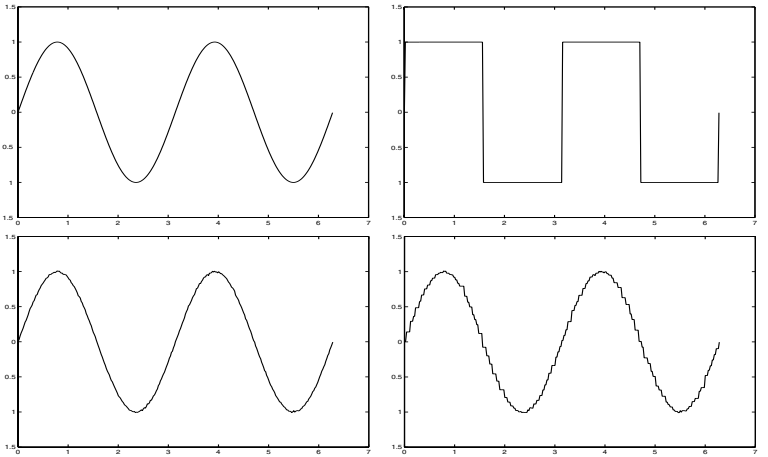

Fig. 1. Signal (sine wave) and its steady state shock filter solution without noise (top) and with very low additive white Gaussian noise, SNR=40dB (bottom).

2 Previous Works

The noise sensitivity problem is critical and unless properly solved - might prevent most practical uses of shock filters. Previous studies addressed the issue suggesting several solutions. The common way seen in literature to increase robustness ([1,3,10,12]) is to convolve the signal's second derivative with a lowpass filter, such as a Gaussian:

$$I_t = -\text{sign}(G_\sigma * I_{xx})|I_x|, \tag{6}$$

where G_σ is a Gaussian of standard deviation σ.

This is generally not sufficient to overcome the noise problem: convolving the signal with a Gaussian of moderate width will in many cases not cancel the inflection points produced by the noise. Their magnitude will be considerably lower, but there will still be a change of sign at these points, which will lead the flow to go in opposite direction at each side. For very wide (large scale) Gaussians - most inflection points produced by the noise are diminished, but at a cost: the location of the signal's inflection points are less accurate. Moreover, the effective Gaussian's width σ is in many cases larger than the length of the signal, thus causing the boundary conditions imposed on the process to strongly affect the solution. Lastly, from a computational point of view, the convolution process in each iteration is costly.

A more complex approach, that we will also follow later, is to address the issue as an enhancing-denoising problem: smoother parts are denoised, whereas edges are enhanced and sharpened. The main idea is to add some sort of anisotropic diffusion term with an adaptive weight between the shock and the diffusion

processes. Alvarez and Mazorra were the first to couple shock and diffusion in [1] proposing an equation of the form:

$$I_t = -\text{sign}(G_\sigma * I_{\eta\eta})|\nabla I| + cI_{\xi\xi} \tag{7}$$

where c is a positive constant and ξ is the direction perpendicular to the gradient ∇I. This equation, though, degenerates to (6) in the 1D case and the diffusion part is lost.

In [10] the process suggested by Kornprobst et al. is:

$$I_t = \alpha_r(h_\tau I_{\eta\eta} + I_{\xi\xi}) - \alpha_e(1 - h_\tau)\text{sign}(G_\sigma * I_{\eta\eta})|\nabla I|, \tag{8}$$

where $h_\tau = h_\tau(|G_{\tilde{\sigma}} * \nabla I|) = 1$ if $|G_{\tilde{\sigma}} * \nabla I| < \tau$, and 0 otherwise. The original scheme has another fidelity term $\alpha_f(I - I_0)$, which can be added to any such schemes, that was omitted here.

In [3] the proposed scheme of Coulon and Arridge is:

$$I_t = \text{div}(c\nabla I) - (1 - c)^\alpha \text{sign}(G_\sigma * I_{\eta\eta})|\nabla I|, \tag{9}$$

where $c = \exp(-\frac{|G_{\tilde{\sigma}} * \nabla I|^2}{k})$. Originally, the process was used for classification, based on a probabilistic framework. Eq. (9) is the adaptation for direct processing on images.

Later we will show examples of these schemes and compare the results to ours.

3 Coupling Shock and Diffusion

In the following section we analyze two discrete schemes involving shock filter and diffusion. We provide a few theorems regarding the behavior of these schemes. The proofs are in Appendix I. For simplicity, our analysis is done in one dimension.

3.1 Shock and Linear Diffusion

We start by adding a linear diffusion term to the shock filter equation:

$$I_t = -\text{sign}(I_{xx})|I_x| + \lambda I_{xx}, \tag{10}$$

where $\lambda > 0$ is a constant weight parameter. The discrete scheme of (10) is:

$$I_i^{n+1} = I_i^n + \Delta t(-\text{sign}(D^2 I_i^n)|DI_i^n| + \lambda D^2 I_i^n), \tag{11}$$

with CFL condition $\lambda\Delta t \leq 0.5h^2$, $(h \leq 1)$.

Theorem 1. *The scheme of (11) obeys the strong minimum-maximum principal (no new local extrema are created and the global maximum and minimum at any time are bounded by those of the initial condition) and reaches a trivial constant steady state solution* $\lim_{n\to\infty} I^n(x) = \text{const}$ *for any* $\lambda > 0$.

This process is a mix between denoising and enhancement processes, where for low λ it behaves more like an enhancing shock filter and for large λ denoising is more dominant (with some edge preservation). Some characteristics of the shock filter are lost: Real shocks are actually not created; the scheme is not total-variation preserving; the signal diminishes with time - the steady state solution is a constant function.

3.2 A TVP Shock and Diffusion Process

An interesting modification of equation (10) is:

$$I_t = -\text{sign}(I_{xx})|I_x| + \lambda I_{xx}|\text{sign}(I_x)|, \tag{12}$$

and its discrete equivalent:

$$I_i^{n+1} = I_i^n + \Delta t(-\text{sign}(D^2 I_i^n)|DI_i^n| + \lambda D^2 I_i^n|\text{sign}(DI_i^n)|). \tag{13}$$

The diffusion term is multiplied by $|\text{sign}(I_x)|$. The value of this expression is always 1 except for the case $I_x = 0$, in which the value is 0. This relatively small change makes an important difference in the behavior of the equation. We should comment that (12) has the most simple shock-diffusion coupling for the sake of straitforward analysis, it is not intended for use on noisy signals.

Theorem 2. *The scheme of (13) is total variation preserving (TVP), local extrema remain unchanged in time and no new local extrema are created.*

Let us define $I^n_{i+\frac{1}{2}}$ as a discrete inflection point if $(D^2 I_i^n)(D^2 I_{i+1}^n) < 0$.

Theorem 3. *If there is a single discrete inflection point between two points of extrema, then its location is preserved through the evolution of (13).*

Theorem 2 implies Eq. (13) can have a nontrivial steady state. Assuming these properties are valid in the continuous domain of Eq. (12) we can simplify the equation locally and calculate in some cases the steady state solution analytically. Here we give an example of how to do it. We consider the case where there is a finite set E of local extrema points of the initial condition $I_0(x) \in C^2$, $x \in [0,1]$. Between every two extrema points there is one inflection point. The calculation of the solution is as follows:

- Let us define by S the set of location of extrema points of $I_0(x)$ and by S_V their value: $S \doteq \{s_1, s_2, .., s_L\} : I_{0x}(s_i) = 0, \quad s_1 < s_2 .. < s_L$, $S_V \doteq \{v_1, v_1, .., v_L\} : v_i = I_0(s_i), \quad 1 < i < L$.
- Let us define by T the set of location of inflection points of $I_0(x)$, $T \doteq \{t_1, t_1, .., t_{L-1}\} : I_{0xx}(t_i) = 0, \quad t_1 < t_2 .. < t_{L-1}$. In this example we assume $0 < s_1 < t_1 < s_2 < .. < t_{L-1} < s_L < 1$.
- Let us define the value at the 2 boundary points $v_0 = I_0(0)$, $v_{L+1} = I_0(1)$ and denote $s_0 = 0$, $s_{L+1} = 1$.

- Following Theorems 2,3 - the location of extrema and inflection points do not change in time. Therefore we can separate the original equation on $x \in [0,1]$ to $2L$ equations with appropriate boundary conditions. Each equation is between an extrema point and an inflection point, except at the boundaries. The $2L$ equations are defined on $[0, s_1], [s_1, t_1], [t_1, s_2], ..[t_{L-1}, s_L], [s_L, 1]$.
- For each equation the first and second derivatives do not change their sign in the entire region. Therefore Eq. (12) can be rewritten at each region as: $I_t = \pm I_x \pm \lambda I_{xx}$ depending on the signs of I_x and I_{xx} at that region. At steady state ($I_t(x) \equiv 0$) at each region the equation reduces to two possible options: $I_x = \pm\lambda I_{xx}$ and the solution is: $I(x) = c_1 \exp(\pm x/\lambda) + c_2$, where c_1, c_2 are arbitrary constants.
- Imposing the following boundary conditions:

$$\begin{aligned} I(s_i) &= v_i & 0 < i < L+1, \\ I(s_i^-) &= I(s_i^+) & 1 < i < L, \\ I(t_i^-) &= I(t_i^+) & 1 < i < L-1, \\ I_x(t_i^-) &= I_x(t_i^+) & 1 < i < L-1, \end{aligned}$$

  We get $4L$ linear equations from the boundary conditions which allow us to calculate the $4L$ constants appearing in the $2L$ equations. Actually there is almost no coupling and we can solve separately every two equations between extrema points, that is on neighboring regions $[s_i, t_i], [t_i, s_{i+1}]$. The two equations on the boundary regions $[0, s_1], [s_L, 1]$ are independent. The weak solution is piece-wise differentiable (for the entire domain $x \in [0,1]$ we get $I(x, t \to \infty) \in C^0$).

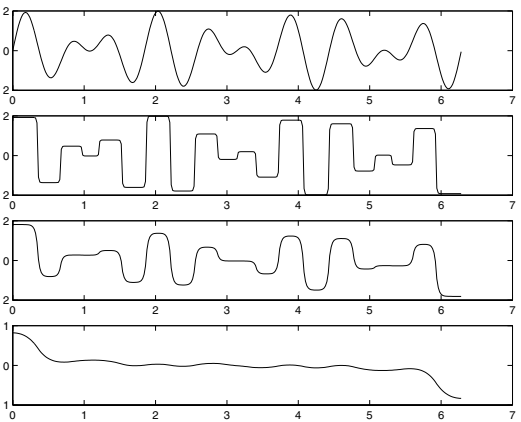

Fig. 2. Three examples of numerical solutions to equation (10) for different values of λ. From top: Initial condition ($I_0 = \sin 7x + \sin 10x$), I(x,t) after 1000 iterations for $\lambda = 0.1, 1, 10$, respectively.

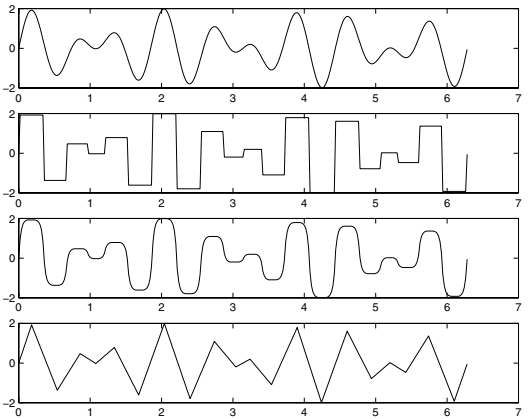

Fig. 3. Three examples of numerical solutions to equation (12) for different values of λ. From top: Initial condition ($I_0 = \sin 7x + \sin 10x$), I(x,t) at steady state for $\lambda = 10^{-4}, 1, 10^4$, respectively.

In Fig. 3 we show the behavior of equation (12) for different values of λ.

3.3 Considering the Second Derivative's Magnitude

in order to account for the magnitude of the second derivative controlling the flow - we return to the original shock filter formulation of (1) and choose $F(s) = \frac{2}{\pi}\arctan(as)$. This function is a "soft" sign, where a is a parameter that controls the sharpness of the slope near zero. The equation is therefore:

$$I_t = -\frac{2}{\pi}\arctan(aI_{xx})|I_x| + \lambda I_{xx}. \tag{14}$$

In this way the inflection points are not of equal weight anymore; regions near edges, with large magnitude of the second derivative near the zero crossing, will be sharpened much faster than relatively smooth regions.

3.4 Incorporating Time Dependency to the Process

Another desirable goal is the ability to change the process behavior with time in a controlled manner. In [5] we elaborate the idea of explicitly incorporating the time t to Perona-Malik type schemes ([13]). The basic idea is that processes controlled by the gradient magnitude have large errors in estimating gradients at the initial stages, where the signal is still very noisy. Therefore a preliminary phase of mainly noise removal can be advantageous. We suggested two processes with continuous transition in time, beginning with linear diffusion at time zero (strong denoising), advancing towards high nonlinearity (strong edge-preserving properties).

Similar ideas can be applied in our case. We would like to decrease the shock affects of the process at the beginning (when estimating the signal's inflection points is difficult) - allowing the diffusion process to smooth out the noise. As the evolution advances, false inflection points produced by the noise are greatly reduced and the enhancing shock part can gain dominance. A simple way to do that is to multiply the second derivative of the shock part by the time t:

$$I_t = -\frac{2}{\pi}\arctan(aI_{xx}t)|I_x| + \lambda I_{xx}. \tag{15}$$

In the next section we give a brief background on complex diffusion. Later we will use this type of process to formulate a new regularized shock filter.

4 Complex Diffusion

4.1 Introduction

Complex diffusion-type processes are encountered i.e. in quantum physics and in electro-optics. In [4] we analyzed a diffusion equation with a complex diffusion coefficient and showed some applications for image filtering. This process is a generalization of the *diffusion equation* and the *time dependent Schrödinger equation* with zero potential. There are little related studies in that field in the vision community. A recent paper by Barbaresco ([2]) presented the closely related issues of calculus of variations in the complex domain and its applications to spectral analysis. In this section we summarize the relevant results of [4].

4.2 Linear Complex Diffusion

Problem Definition. Let us consider the following initial value problem:

$$\begin{aligned} I_t &= cI_{xx}, \qquad t > 0, \qquad x \in \mathbb{R} \\ I(x;0) &= I_0 \in \mathbb{R}, \quad c, I \in \mathbb{C}. \end{aligned} \tag{16}$$

We rewrite the complex diffusion coefficient as $c \doteq re^{i\theta}$, and, since there does not exist a stable fundamental solution of the inverse diffusion process, restrict ourselves to a positive real value of c, that is $\theta \in (-\frac{\pi}{2}, \frac{\pi}{2})$.

The fundamental solution is:

$$h(x;t) = G_\sigma(x;t)e^{i\alpha(x)}, \tag{17}$$

where

$$\alpha(x) = \frac{x^2 \sin\theta}{4tr}, \quad \sigma(t) = \sqrt{\frac{2tr}{\cos\theta}}. \tag{18}$$

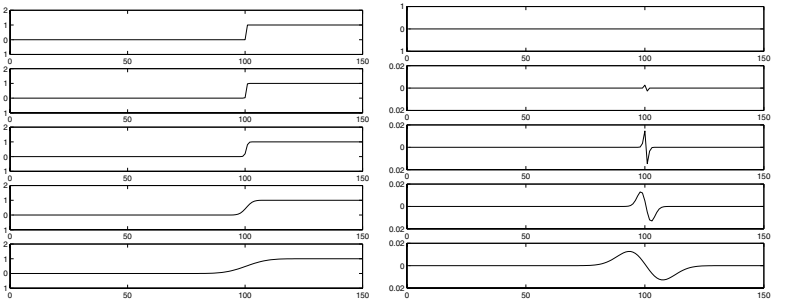

Fig. 4. Complex diffusion of a small theta applied to a step signal ($\theta = \pi/30$). Left - real values, right - imaginary values. Each frame depicts from top to bottom: original step, diffused signal after times: 0.025, 0.25, 2.5, 25.

Fig. 5. Complex diffusion of the cameraman image for small theta ($\theta = \pi/30$) after 10 iterations. Left - real values, right - imaginary values (factored by 20).

Approximate Solution for Small Theta. We showed in our previous study that as $\theta \to 0$ the imaginary part can be regarded as a smoothed second derivative of the initial signal, factored by θ and the time t. Generalizing the solution to any dimension with Cartesian coordinates $\mathbf{x} \doteq (x_1, x_2, ..x_N) \in \mathbb{R}^N$, $I(\mathbf{x}; t) \in \mathbb{C}^N$ and denoting that in this coordinate system $\mathbf{G}_\sigma(\mathbf{x}; t) \doteq \prod_i^N G_\sigma(x_i; t)$, we get:

$$\lim_{\theta \to 0} \frac{Im(I)}{\theta} = t \Delta \mathbf{G}_{\hat{\sigma}} * I_0, \tag{19}$$

where $Im(\cdot)$ denotes the imaginary value and $\hat{\sigma} = \sqrt{2t}$.

In Figs. (4), (5) 1D and 2D examples are shown of the complex diffusion evolution process for small θ. The edge detection (smoothed second derivative) properties are clearly apparent in the imaginary part, whereas the real value depicts the properties of ordinary Gaussian scale-space.

4.3 Nonlinear Complex Diffusion

Nonlinear complex processes can be derived from the above mentioned properties of the linear complex diffusion for purposes of signal and image denoising or enhancement. Numerical evidence show that the qualitative characteristics of the imaginary part in nonlinear processes are similar to the linear case, especially at the zero-crossing locations. In [4] a nonlinear ramp denoising process is presented.

5 Complex Shock Filters

From (15) and (19) we derive the complex shock filter formulation:

$$I_t = -\frac{2}{\pi}\arctan(a\mathrm{Im}(\frac{I}{\theta}))|I_x| + \lambda I_{xx}, \tag{20}$$

where $\lambda = re^{i\theta}$is a complex scalar. Implementation of equation (20) is done by the same discrete approximations (except that all computations are complex); the CFL condition in 1D is $\Delta t \leq 0.5h^2\frac{\cos\theta}{r}$.

The complex shock filter generalization to 2D is:

$$I_t = -\frac{2}{\pi}\arctan(a\mathrm{Im}(\frac{I}{\theta}))|\nabla I| + \lambda I_{\eta\eta} + \tilde{\lambda} I_{\xi\xi}, \tag{21}$$

where $\tilde{\lambda}$ is a real scalar.

The complex filter is an elegant way to avoid the need of convolving the signal in each iteration and still get smoothed estimations. The time dependency of the process is inherent, without the need to explicitly use the evolution time t. Moreover, the imaginary value receives feedback - it is smoothed by the diffusion and enhanced at sharp transitions by the shock, thus can serve better for controlling the process then a simple second derivative.

In Fig. 6 a noisy sine wave is processed by several shock-filter based processes described earlier. The original shock filter (Eq. (2)) and the one with Gaussian convolved second derivative (Eq. (6)) are clearly not suitable for this task. The process of Kornprobst et al. (Eq. (8)) performs relatively well but the minimum and maximum of the signal decay quite fast and the deblurring is not so strong. Moreover there are 5 parameters that need to be adjusted and from our experience the performance of the process is quite sensitive to a few of them (esp. to τ). The process of Coulon and Arridge (Eq. (9)) behaves somewhat better in this 1D example, it produces shock structures but is strongly affected by to the boundary conditions and tends to move the shocks towards the center. Our complex shock filter scheme (Eq. (20)) seems to produce the best result, compared to the ideal result shown at the top right. The scheme is stable in time, decays slowly and preserves well the location of the shocks. Another advantage of our scheme is that we basically have only two parameters: $|\lambda|$ and a (in the 1D case, three in 2D). Note: as the process is normalized - it is not affected by the exact value of θ as long as it is small. In all our experiments we took $\theta = 0.01$. At the bottom right we can see the imaginary value of the complex process (the scale

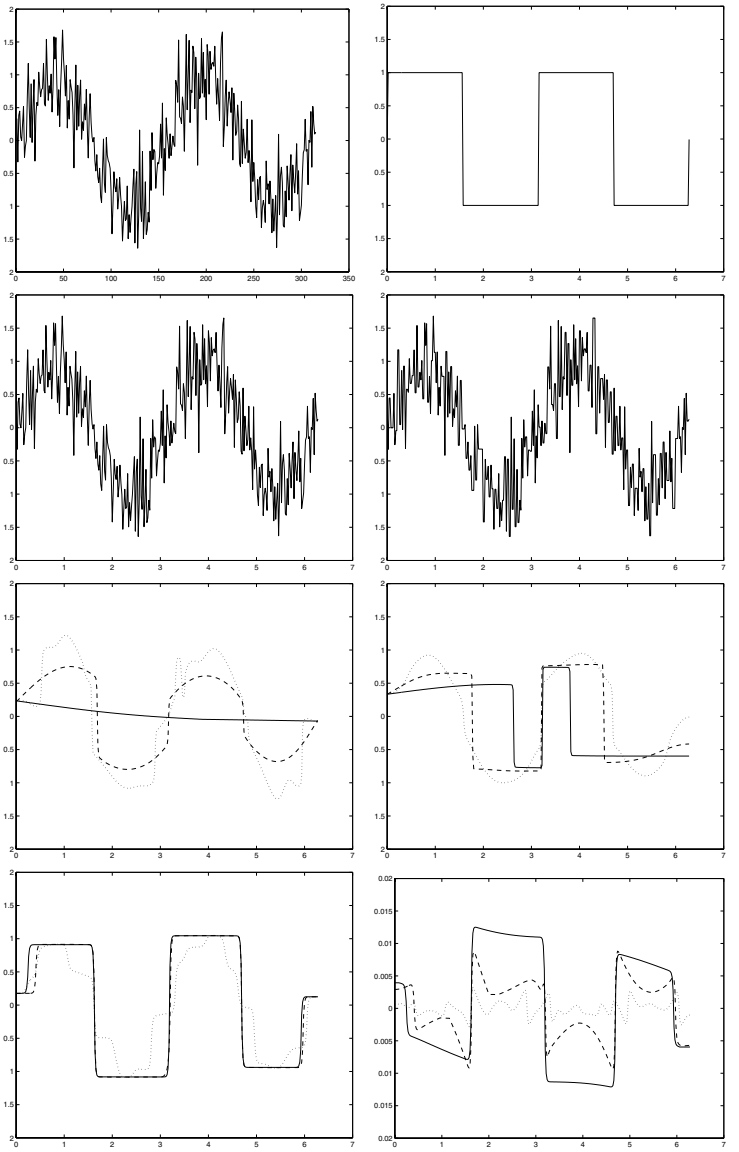

Fig. 6. Noisy signal (sine wave) processed by several algorithms. From top, left: signal with additive white Gaussian noise (SNR=5dB), right: ideal steady state shock result; left: steady state of original shock filter Eq. (2), right: steady state of Eq. (6) - Gaussian convolved derivative, $\sigma = 100$; left: evolution of Eq. (8) - Kornprobst et al. ($\alpha_r = 1, \alpha_e = 0.5, \tau = 0.04, \sigma = 30, \tilde{\sigma} = 5$), right: evolution of Eq. (9) - Coulon-Arridge ($k = 0.01, \alpha = 1, \sigma = 30, \tilde{\sigma} = 5$); bottom: evolution of Eq. (20) - complex shock filter (our proposed scheme), left: real values, right: imaginary values, ($|\lambda| = 0.5, a = 5$). All evolution graphs depict 3 time points along the evolution: 300 (dotted), 3,000 (dashed) and 30,000 (solid) iteration.

is 100 times smaller). One can see that the zero crossings are at the inflection points and that the imaginary value energy grows with time - thus enabling good preservation of the shocks.

In Fig. 7 a blurred and noisy tools image is processed. In the two dimensional case only the schemes of Kornprobst et at. and our complex scheme have acceptable results at this levels of noise. Though, the complex process have sharper edges and is closer to the shock process (as can be seen in comparison to ideal shock response, for a blurred image without noise - top right). At the bottom right a plot of one horizontal line of the image shows the denoising achieved by the complex scheme along with sharper large edges.

6 Conclusion

Some processes based on the shock and diffusion equations were presented. The paper focused on reducing the inherent noise sensitivity of the shock filter in order to allow more practical uses of it. We analyzed the coupling of shock and linear diffusion in the discrete domain, showed that the process converges to a trivial constant steady state and suggested a modification for a total variation preserving scheme. For the purpose of regularizing the shock filter our suggestion is to add a complex diffusion term and to use the imaginary value as the controller for the direction of the flow instead of the second derivative. This results in a robust and stable deblurring process that can still be effective in noisy environments.

Acknowledgments. This research has been supported in part by the Ollendorf Minerva Center, by the Fund for the Promotion of Research at the Technion, by the Israeli Ministry of Science, Israeli Academy of Science and by the Technion V.P.R. Fund.

APPENDIX I

Proof of Theorem 1

All lemmas refer to the evolution of Eq. (11). I_i^n is a discrete signal of N points $(1 \leq i \leq N)$ at iteration n.

Lemma 1. *If* $(I_i^n \geq I_{i+1}^n$ *and* $I_i^n > I_{i-1}^n)$ *or* $(I_i^n > I_{i+1}^n$ *and* $I_i^n \geq I_{i-1}^n)$ *then* $I_i^{n+1} < I_i^n$.

Proof. From the definition of the minmod function it follows that $DI_i^n = 0$. From (5) $D^2 I_i^n < 0$ and therefore $I_i^{n+1} = I_i^n + \Delta t(\lambda D^2 I_i^n) < I_i^n$.

Lemma 2. *If* $I_i^n = I_{i-1}^n = I_{i+1}^n$ *then* $I_i^{n+1} = I_i^n$.

Proof. $DI_i^n = 0$, $D^2 I_i^n = 0$.

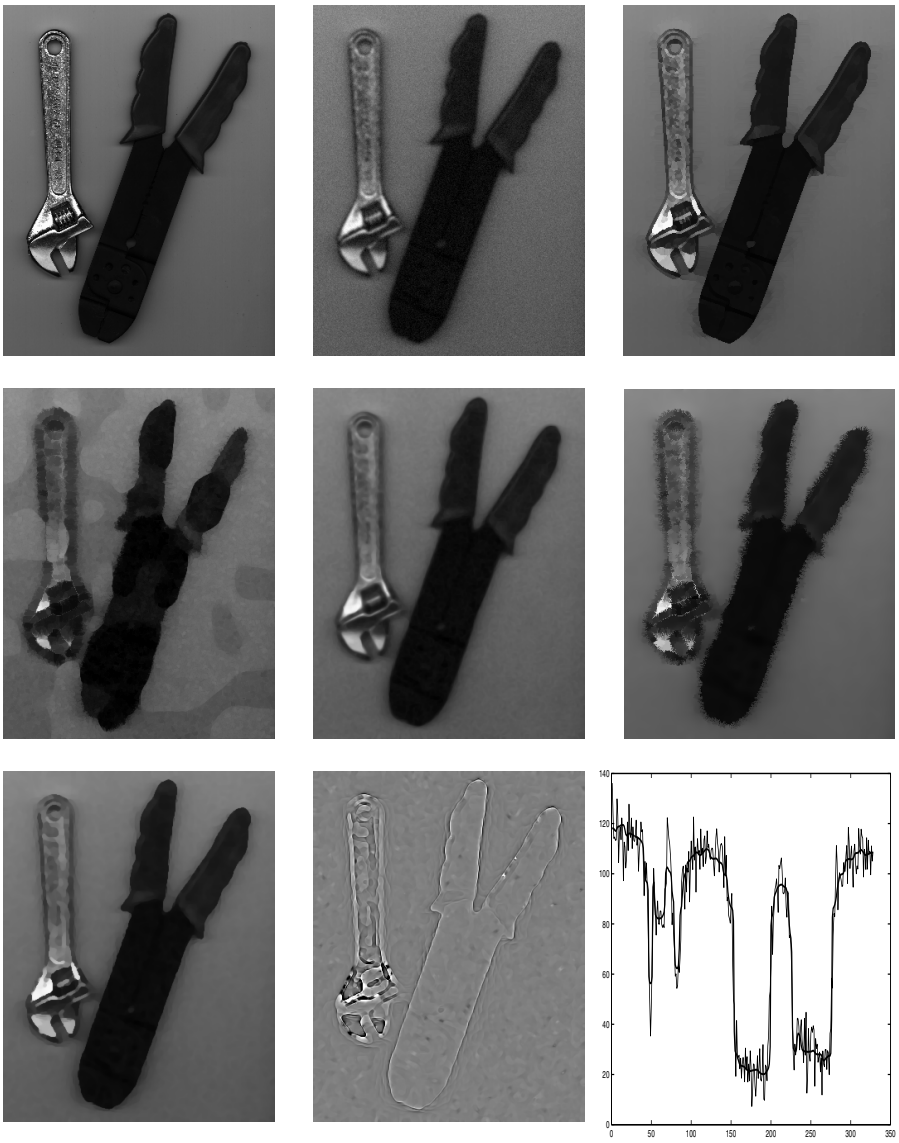

Fig. 7. Top row (from left): Original tools image, Gaussian blurred ($\sigma = 2$) with added white Gaussian noise (SNR=15dB), ideal shock response (of blurred image without the noise); middle row: evolutions of Eq. (7) - Alvarez-Mazorra ($\sigma = 10$), Eq. (8) - Kornprobst et al. ($\alpha_r = 0.2, \alpha_e = 0.1, \tau = 0.2, \sigma = 10, \tilde{\sigma} = 1$), Eq. (9) - Coulon-Arridge ($k = 5, \alpha = 1, \sigma = 10, \tilde{\sigma} = 1$); bottom: evolution of Eq. (20) - complex process, left: real values, middle: imaginary values ($|\lambda| = 0.1, \tilde{\lambda} = 0.5, a = 0.5$), right: one horizontal line showing the gray level values of the complex evolution (thin line - iteration 1, bold line - iteration 100). All evolution results are for 100 iterations, dt=0.1.

Lemma 3. *The value of any maximum point I_i^n where $I_{i-M_1}^n < I_{i-M_1+1}^n = .. = I_i^n = .. = I_{i+M_2-1}^n > I_{i+M_2}^n$ will be reduced after $\min(M_1, M_2)$ steps, that is: $I_i^{n+\min(M_1,M_2)} < I_i^n$.*

Proof. Let us assume $M_1 = \min(M_1, M_2)$, without loss of generality (wlog). Following Lemma 1 $I_{i-M_1+1}^{n+1} < I_{i-M_1+1}^n$. Following Lemma 2 $I_i^{n+1} = I_i^n$. We can repeat this $M_1 - 1$ steps until $I_{i-1}^{n+M_1-1} < I_{i-1}^{n+M_1-2} = I_i^n$. Then the conditions of Lemma 2 are not holding anymore and following Lemma 1 we get $I_i^{n+M_1} < I_i^{n+M_1-1} = I_i^n$.

Lemma 4. *At the boundary points: If $I_1^n > I_2^n$ then $I_1^{n+1} < I_1^n$; if $I_N^n > I_{N-1}^n$ then $I_N^{n+1} < I_N^n$.*

Proof. Let us examine the point I_1^n. The Neumann BC dictates $DI_1^n = 0$. This condition is equivalent to extending the signal (to $i = 0$) and setting $I_0^n \equiv I_1^n$ for any n. Thus $D^2 I_1^n$ is well defined. As $I_1^n > I_2^n$ we get $D^2 I_1^n < 0$ and therefore $I_1^{n+1} < I_1^n$. Similar arguments are valid for the boundary point I_N^n.

Theorem 1

Proof. From Lemma 3 any local maximum point decreases after a finite number of steps. Similarly, it can be shown that any local minimum point increases after a finite number of steps. At steady state $I_i^{n+M} = I_i^n$ for any positive integer M, therefore it contains no local extrema. Lemma 4 forbids the maximum or minimum to be at the boundaries at steady state. We conclude that the only possible steady state solution is a constant function.

Proof of Theorem 2

All lemmas refer to the evolution of Eq. (13).

Lemma 5. *If I_i^n is an extrema point then $I_i^{n+1} = I_i^n$.*

Proof. Let us assume I_i^n is a maximum point: $I_i^n \geq I_{i-1}^n, I_{i+1}^n$. Therefore $DI_i^n = 0$ and we get $I_i^{n+1} = I_i^n$. The same applies for minimum points.

Lemma 6. *If I_i^n is a maximum/minimum point then I_i^{n+1} is a maximum/minimum point.*

Proof. Let us assume I_i^n is a maximum point: $I_i^n \geq I_{i-1}^n, I_{i+1}^n$. We should prove the relations at the next step are: $I_i^{n+1} \geq I_{i-1}^{n+1}, I_{i+1}^{n+1}$. We examine the point I_{i-1}^n. There are two possible cases: if I_{i-1}^n is an extrema point itself, then by Lemma 5 it is not changed and we have $I_i^{n+1} = I_i^n \geq I_{i-1}^n = I_{i-1}^{n+1}$. If I_{i-1}^n is not an extrema point then $I_i^n > I_{i-1}^n > I_{i-2}^n$, $DI_{i-1}^n \neq 0 \Rightarrow |\text{sign}(DI_{i-1}^n)| = 1$ and we get: $I_{i-1}^{n+1} = I_{i-1}^n + \Delta t[|I_{i-1}^n - I_i^n|/h + (I_i^n - 2I_{i-1}^n + I_{i-2}^n)/h^2]$. The last term $((..)/h^2)$ is negative. using the CFL relation: $\Delta t \leq 0.5h^2 \leq 0.5h$ for any $h \leq 1$ we get $I_{i-1}^{n+1} < I_{i-1}^n + 0.5(I_i^n - I_{i-1}^n) = 0.5(I_i^n + I_{i-1}^n) < I_i^n = I_i^{n+1}$. The same can be proven for I_{i+1}^{n+1} and similar arguments hold for minimum points.

From Lemmas 5,6 it follows that extrema points are stable and their value does not change through the evolution process. As extrema points are unchanged and no new local extrema are created - the scheme is TVP.

Theorem 3

The proof of this theorem is somewhat more lengthy and will appear in our technical report ([7]). The intuition behind it is that near inflection points the diffusion is weaker than the shock. Therefore in the evolution process there will be a point where $|D^2I| < |DI|$ and the shock will prevent the inflection point from being vanished or moved.

References

1. L. Alvarez, L. Mazorra, "Signal and image restoration using shock filters and anisotropic diffusion", SIAM J. Numer. Anal. Vol. 31, No. 2, pp. 590-605, 1994.
2. F. Barbaresco, "Calcul des variations et analyse spectrale: equations de Fourier et de Burgers pour modeles autoregressifs regularises", Traitement du Signal, vol. 17, No. 5/6, 2000.
3. O. Coulon, S.R. Arridge, "Dual echo MR image processing using multi-spectral probabilistic diffusion coupled with shock filters", MIUA'2000, British Conference on Medical Image Understanding and Analysis, London, United-Kingdom, 2000.
4. G. Gilboa, Y.Y. Zeevi, N. Sochen, "Complex diffusion processes for image filtering", Michael Kerckhove (Ed.): Scale-Space 2001, LNCS 2106, pp. 299-307, Springer-Verlag 2001.
5. G. Gilboa, N. Sochen, Y.Y. Zeevi, "Image enhancement segmentation and denoising by time dependent nonlinear diffusion processes", ICIP-'01, Thessaloniki, Greece, October 2001.
6. G. Gilboa, N. Sochen, Y.Y. Zeevi, "Anisotropic selective inverse diffusion for signal enhancement in the presence of noise", Proc. IEEE ICASSP-2000, Istanbul, Turkey, vol. I, pp. 211-224, June 2000.
7. G. Gilboa, N. Sochen, Y.Y. Zeevi, "Complex diffusion for image filtering", CCIT Technical Report, Technion-IIT, Haifa, Israel - to appear.
8. F. Guichard, J-M. Morel, "A note on two classical shock filters and their asymptotics", M. Kerckhove (Ed.): Scale-Space 2001, LNCS 2106, pp. 75-84, Springer-Verlag 2001.
9. M. Kerckhove (Ed.), "Scale-Space and morphology in computer-vision", Scale-Space 2001, LNCS 2106, Springer-Verlag 2001.
10. P. Kornprobst, R. Deriche, G. Aubert, "Image coupling, restoration and enhancement via PDE's", Proc. Int. Conf. on Image Processing 1997, pp. 458–461, Santa-Barbara (USA), 1997.
11. S.J. Osher and L. I. Rudin, "Feature-oriented image enhancement using shock filters", SIAM J. Numer. Anal. 27, pp. 919-940, 1990.
12. N.Rougon, F.Preteux, "Controlled anisotropic diffusion", Proc. SPIE Conf. on Nonlinear Image Processing VI - IS&T / SPIE Symp. on Electronic Imaging, Science and Technology '95, San Jose, CA, Vol. 2424, 1995, pp. 329-340.
13. P. Perona and J. Malik, "Scale-space and edge detection using anisotropic diffusion", IEEE Trans. PAMI, vol. PAMI-12,no. 7, pp. 629-639, 1990.
14. B M ter Haar Romeny Ed., "Geometry driven diffusion in computer vision", Kluwer Academic Publishers, 1994.